Synthesis and Characterization of Expanded Smectites Containing Trinuclear Co Complexes

S. M. Thomas,[†,‡] J. A. Bertrand,[‡] M. L. Occelli,*[,†] J. M. Stencel,[§] and S. A. C. Gould[||]

GTRI, Zeolites and Clays Program, Georgia Institute of Technology, Atlanta, Georgia 30332-0827; Department of Chemistry & Biochemistry, Georgia Institute of Technology, Atlanta, Georgia 30332-0400; Center for Applied Energy Research, Lexington, Kentucky 40511; and W. M. Keck Science Center, Claremont Colleges, Claremont, California 91711

Received December 7, 1998. Revised Manuscript Received February 16, 1999

Several smectites were pillared with metal complexes, such as the trimeric cobalt cation $[Co_3(OC_2H_4NH_2)_6]^{3+}$ and its divalent analogue $[Co_3(OC_2H_4NH_2)_6]^{2+}$, containing clusters of one to three cobalt cations separated by bridging ligands. In pillared interlayered clays (PILC) prepared by reacting Na−montmorillonite with $Co_3(H_2NCH_2CH_2O)_6(ClO_4)_3$ solutions, pillar orientation is controlled by the trimer concentration in the interlamellar space. Initially the Co trimer (0.72 nm × 0.48 nm in size) lies parallel to the clay surface. Then as more trimer is introduced, it forms an angle of ∼48° relative to the clay surface that increases to 61° as the clay reached its highest Co loadings. FT IR and FT LRS spectra together with chemical analysis have been used to ascertain the presence of pristine trimer ions in all the PILC samples. XPS results indicate that reduction of the trivalent trimer to its divalent analogue $[Co_3(OC_2H_4NH_2)_6]^{2+}$ has occurred during PILC preparation. XRD patterns and molecular scale AFM images have revealed the presence of trimer molecules also on the clay external surface. Thermogravimetric analyses of $[Co_3(OC_2H_4NH_2)_6]^{3+}$ PILC are all qualitatively similar despite the variance in *d* spacing seen at different Co trimer loadings. Ligand decomposition occurs in two steps in the 250−450 °C temperature range. At $T >$ 250 °C, ligand losses cause a total structural collapse of the pillared structure. In contrast, prior to 250 °C, the interlamellar expansion decreases and the trimer seems to adopt a position parallel to the clay surface. The *d* spacing changed very little over the temperature range where initial ligand losses occur. Partial decomposition of the trimeric complex can thus be achieved while a 0.45 nm layer expansion is maintained, indicating that these materials could be considered as cobalt catalysts for low temperature ($T <$ 200 °C) applications.

Introduction

Long before there was an understanding of the scientific basis of their properties, clays enjoyed wide practical uses as clarifiers for alcoholic beverages and as decolorizers for edible oils.[1,2] The practice of mixing raw wool with an aqueous slurry of clays (known as fuller's earth) to remove grease dates back to antiquity. In the 1930s, at the time when the cracking properties of clays were first discovered and reported,[3] the concept of clays as crystalline materials composed of silicate layers became generally accepted.[4] In the late 1950s, Barrer and co-workers[5,6] realized that it was possible to ion exchange charge-compensating cations in these crystalline materials with large quaternary ammonium cations and generate microporous structures with surface areas available to sorption and catalysis. The properties of this type of microporous materials have been reported in several review papers.[7−10] The properties and structures of pillared interlayered clays (PILC) have been discussed in the references given.[11,12]

The low thermal stability of the organic pillars is not a limiting consideration when studying and using these

* Corresponding author.
† Zeolites and Clays Program, Georgia Institute of Technology.
‡ Department of Chemistry & Biochemistry, Georgia Institute of Technology.
§ Center for Applied Energy Research.
|| W. M. Keck Science Center, Claremont Colleges.

(1) Grim, R. E. *Applied Clay Minerology*; McGraw-Hill: New York, 1962.
(2) Siddiqui, M. K. H. *Bleaching Earths*; Pergamon Press: Oxford, 1968.
(3) Marshall, S. *Petr. Refin.* **1952**, *3*, *9*, 263.
(4) Pauling, L. *Proc. Natl. Acad. Sci. U.S.A.* **1930**, *16*, 129 and 578−82.
(5) Barrer, R. M. *Zeolites and Clay Minerals as Sorbents and Molecular sieves*; Academic Press: New York, 1968.
(6) Barrer, R. M.; MacLeod, D. M. *Trans. Faraday Soc.* **1955**, *51*, 1290.
(7) Pinnavaia, T. J. *Science* **1983**, *220*, *4595*, 365.
(8) Figueras, J. *Catal. Rev., Sci., Eng.* **1988**, *30*, *3*, 457.
(9) Occelli, M. L. In *Keynotes in Energy Related Catalysis*; Kaliaguin, S., Ed.; Elsevier: 1988; Chapter 2, p 101.
(10) Corma, A. *Chem. Rev.* **1995**, *95*, 559.
(11) Brindley, G. W., Brown, G., Eds. *Crystal Structure of Clay Minerals & Their X-ray Identification*, 3rd ed.; Mineral Society: London, 1980.
(12) Brown, G., Ed. *The X-ray Identification and Crystal Structures of Clay Minerals*, 2nd ed.; Mineral Society: London, 1961.

10.1021/cm9811141 CCC: $18.00
Published on Web 03/25/1999

microporous solids for fine chemicals preparation at low (<100 °C) reaction temperatures in place of homogeneous catalysts. Initial studies focused on the ion-exchange of the clay charge-compensating cations with simple organic species such as tetraalkylammonium ions.[6] More swell-resistant materials with larger pore openings were synthesized when rigid or cagelike amines such as 1,4-diazabicyclo[2,2,2]octane[13,14] were used as intercalants. These polycationic species were found capable of simultaneously interacting with the two interlamellar surfaces of the clay, generating in this way cross-linked smectites (CLS) with improved stability.[13] These expanded clays found utility as low-temperature catalysts for the esterification of carboxylic acids.[15,16] Metal complexes typically used as homogeneous catalysts were also intercalated into clays and often demonstrated improved selectivity over their solution counterparts.[17−19] Some well-known cationic compounds used to expand clays can be found in refs 20−30.

Diels−Alder, Friedel−Crafts, and Michael addition reactions are but a few examples of commercially important organic syntheses catalyzed by metal-promoted montmorillonites.[31] Catalytic activity and liquid product selectivity in the aforementioned reactions depends on the type and nature of the cations present in the clay interlamellar space. The purpose of this paper is to report the synthesis and characterization of montmorillonites expanded with cationic polynuclear Co complexes.

The cobalt series consists of mononuclear, dinuclear, and trinuclear species with the metal(s) octahedrally coordinated by aminoethanol ligands. The focus of the research will be on the $[Co_3(OC_2H_4NH_2)_6]^{3+}$ ion. The structure of the perchlorate salt of this trinuclear (Co_3) ion was determined and it consists of two *fac*-tris(2−aminoethoxido)cobalt(III) complexes each sharing three oxygens with a central Co(III) ion for which the coordination is distorted octahedral;[32] see Figure 1. The structure of the corresponding ion with a +2 charge was originally studied as the acetate salt and was reported to have a central Co(II) ion with trigonal prismatic coordination.[33] That structure has been reinvestigated[34] and found to contain disordered complexes with octahedral coordination of the central ion. Distorted octahedral coordination of the central ion has also been found for the hexafluorophosphate (PF_6^{-1}) salt of the divalent ion.[32] The syntheses of several Co complexes have been described in detail elsewhere.[33,35,36]

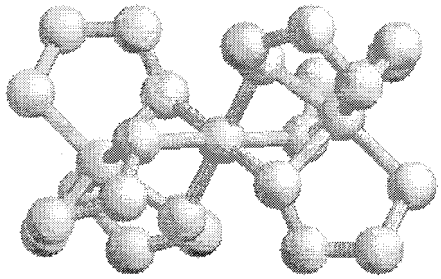

Figure 1. Schematic representation of the $[Co_3(OC_2H_4NH_2)_6]^{3+}$ structure.

Experimental Section

Materials. Samples of Bentolite H, (Na−bentonite) and Bentolite L, (Ca−bentonite) were obtained from the Southern Clay Products, Inc. (Gonzales, TX) and were certified to contain >90% montmorillonite. Natural hectorite was supplied in spray-dried form by the Industrial Chemicals Division of NL Industries. The received minerals contained quartz, dolomite, and calcite impurities. Before expanding these clays, attempts were made to remove their impurities using traditional sedimentation methods. Other clays such as synthetic Laponite, obtained from Laporte Industries, and synthetic saponite, provided by Kunimine Industries Co., Ltd. of Japan, were used without further purification; these samples have been described in detail elsewhere.[35,36] Molecular formulas for these clay minerals can be determined from elemental analysis data using methods described elsewhere.[36] Calculated unit cell compositions and layer charges are given in Table 1. Because of impurities, unit cell calculations were not performed for the hectorite sample.

Pillaring Solutions Preparation. Pillaring solutions were prepared using different solvents, such as acetonitrile (ACN), methanol, and water, to dissolve the various Co complexes. $[Co_3(H_2NCH_2CH_2O)_6](ClO_4)_3$ crystals were prepared by dissolving 5.0 g of Co(II) acetate hydrate in 50 mL of methanol. In a separate container, 3.6 g of 2-aminoethanol was mixed with 5 mL of methanol and slowly added to the first solution. Air was bubbled through the solution at room temperature for 1 h. The solution was heated to boiling and 1.2 g of potassium hydroxide dissolved in methanol was slowly added. The mixture was stirred for 5 min and then allowed to cool in an ice bath to form a red precipitate. The solid was filtered, washed, and dried in a vacuum desiccator. The red powder was suspended in 50 mL of methanol and 15 mL of 30% hydrated lithium perchlorate, dissolved in 25 mL of methanol, was added to the resultant dark brown solution. After cooling in an ice bath for 1 h, a brown solid was recovered.

The acetate salt $[Co_3(H_2NCH_2CH_2O)_6](CH_3CO_2)_2$ was prepared according to a procedure developed by Bertrand.[32] The

(13) Shabtai, J.; Frydman, N.; Lazar, R. *Proceedings of the 6th International Congress on Catalysis, London, 1976*; Bond, G. C., Wells, P. B., Tompkins, F. C., Eds.; The Chemical Society: London, 1976; p 660.
(14) Mortland, M. M.; Berkheiser, V. *Clays Clay. Miner.* **1976**, *24*, 60.
(15) Cabrera, A.; Vazquez, D.; Velasco, L.; Salmon, M.; Arias, J. L. *J. Mol. Catal.* **1992**, *75*, 101.
(16) Lin, C.; Pinnavaia, T. J. *Chem. Mater.* **1991**, *3*, 213.
(17) Giannelis, E. P.; Rightor, E. G.; Pinnavaia, T. J. *J. Am. Chem. Soc.* **1988**, *110*, 3880.
(18) Pinnavaia, T. J.; Welty, P. K. *J. Am. Chem. Soc.* **1975**, *97*, *13*, 5619.
(19) Pinnavaia, T. J.; Raythatha, R.; Lee, J., Halloran, L. J.; Hoffman, J. F. *J. Am. Chem. Soc.* **1979**, 6891.
(20) Krenske, D.; Abdo, S.; Van Damme, H.; Cruz, M.; Fripiat, J. J. *J. Phys. Chem.* **1980**, *84*, 2447.
(21) Van Damme, H.; et al. *J. Mol. Catal.* **1984**, *27*, 123.
(22) Farzaneh, F.; Pinnavaia, T. J. *Inorg. Chem.* **1983**, *22*, 2216.
(23) Pinnavaia, T. J. *ACS Symp. Ser.* **1982**, *192*, 241.
(24) Raythatha, R.; Pinnavaia, T. J. *J. Organomet. Chem.* **1981**, *218*, 115.
(25) Barrer, R. M.; Jones, D. L. *J. Chem. Soc. A* **1970**, 1531.
(26) Shabtai, J.; et al. *Chim. Ind.* **1979**, *61*, 734.
(27) Traynor, M. F.; et al. *Clays & Clay Min.* **1978**, *26*, 318.
(28) Berkheiser, V. E.; Mortland, M. M. *Clays Clay Miner.* **1977**, *25*, 105.
(29) Fraile, J. M.; Garcia, J. I.; Mayoral, J. A. *Chem. Commun.* **1996**, 1319.
(30) Barrer, R. M. *Clays Clay Miner.* **1989**, *37*, *5*, 385.
(31) Izumi, Y.; Urabe, K.; Onaka, M. In *Zeolites, Clays and Heteropoly Acid in Organic reactions*; Kodansha Ltd.: Tokyo, Japan, 1992.
(32) Bertrand, J. A. Unpublished work.
(33) Bertrand, J. A.; Kelly, J. A.; Vassian, E. G. *J. Am. Chem. Soc.* **1969**, *91*, 9, 2394.
(34) Bino, A. Hibrew University, Tel Aviv, personal communication to J. A. Bertrand.
(35) Bertrand, J. A.; Eller, P. G.; Fujita, E.; Lively, M. O.; Van Derveer, D. G. *Inorg. Chem.* **1979**, *18*, 2419.
(36) Thomas, S. Ph.D dissertation. GIT, Atlanta, GA, 1997.

Table 1. Unit Cells and Layer Charges of the Clay Samples under Study[1]

clay mineral	unit cell formulas calculated from elemental analysis data	charge/unit cell
Na−mont	$[(Si_{8.0})(Al_{3.02}Mg_{0.50}Ca_{0.06}Fe_{0.18}Ti_{0.02}\,Na_{0.22})O_{20}(OH)_4]Na_{0.97}K_{0.01}$	0.98
Ca−mont	$[(Si_{8.0})(Al_{2.74}Mg_{0.82}Ca_{0.36}Fe_{0.04}Ti_{0.04})O_{20}(OH)_4]Na_{0.06}Ca_{0.08}K_{0.01}$	1.14
Laponite	$[(Si_{7.72}Mg_{0.28})(Li_{0.58}Mg_{5.42})O_{20}(OH)_{1.56}(F)_{2.44}]Na_{.97}Li_{0.16}$	0.98
saponite	$[(Si_{7.88}Al_{0.12})(Al_{0.22}Mg_{5.24}Ca_{0.10}Na_{0.44})O_{20}(OH)_4]Na_{0.29}$	0.34

procedure by Gerasenkova et al.[37] was used to prepare $[Co_2(H_2NCH_2CH_2O)_3(H_2NCH_2CH_2OH)_3](NO_3)_3$ crystals while the preparation of the monomer, $Co(H_2NCH_2CH_2O)_3{\cdot}3H_2O$, was based on a synthesis procedure published by Evreev.[38]

Pillared Clays Preparation. Pillared Ca− or Na−montmorillonites were prepared using similar procedures. A 35.0 g sample of clay was suspended in 1.0 L of acetonirile, and 8.36 g of cobalt trimer salt $[Co_3(H_2NCH_2CH_2O)_6](ClO_4)_3$ was placed in a Soxhlet cup. The ACN/clay slurry was stirred, at boiling, until the solvent exhibited a red tint, indicating the presence of the complex in solution. The pillared clay was filtered, washed with 100 mL of hot solvent, reslurried with 200 mL of solvent, filtered, and washed again with hot solvent until a colorless filtrate was obtained. The resulting Co_3−PILC was air-dried for 24 h and then oven-dried at 100 °C for 8 h; dark-peach powders were obtained.

Natural hectorite and Laponite were pillared using similar procedure employing 8.36 g of trimer/g of clay and a Soxhlet extraction period of 72 h. Because of its lower cation exchange capacity , saponite was pillared with only 4.19 g of trimer/g of clay and using a Soxhlet extraction period of 2 weeks. Montmorillonites were also pillared with other salts such as $[Co_3(H_2NCH_2CH_2O)_6](CH_3CO_2)_2$, $[Co_2(H_2NCH_2CH_2O)_3(H_2NCH_2CH_2OH)_3](NO_3)_3$, and $Co(H_2NCH_2CH_2O)_3{\cdot}3H_2O$. ACN solutions containing 0.25−1.0 mequiv of salt/g of clay were also used. When using the acetate or the neutral salt, 0.5−0.65 mequiv of ethylene glycol/g of clay was used as a wedging agent to facilitate the exchange reaction. Details of the synthesis of these materials can be found elsewhere.[36]

Powder XRD. All powder X-ray diffraction work was performed on a Rigaku geigerflex XRD CN2155*6 instrument with a 1.2 kW generator, a sealed tube, and a line-focused Cu target with monochromator controlled by a Rigaku DMAXB with version 3.0 software. All scans were continuous with a data collection rate of 0.5°/min and a sampling interval of 0.05 s. All samples were oven-dried at 100 °C for 30 min before being pressed (to avoid orientation) onto glass lids.

Elemental Analysis. Metal analysis was performed by Applied Technical Services, Inc. using atomic absorption. Carbon, nitrogen, and halide analysis was done by Atlantic Microlab. Acid digestion was used to dissolve the pillared materials. Carbon and nitrogen analyses were determined by combustion. Halide analysis was determined by ash test. Trace amounts (<0.05%) of elements were not reported.

Thermogravimetric Analysis. All thermogravimetric analyses (TGA and DTA) were obtained on a Seiko 210/310 analyzer equipped with 3.0 version software or a Perkin-Elmer 7.0 analyzer. Compressed nitrogen or air was introduced with a flow rate of 80 mL/min. Samples were heated at a rate of 10.0 °C/ min up to 100 °C. The temperature was held constant for all pillared clay samples for 30 min, to induce the loss of adsorbed water and solvent, and then heated at a rate of 5.0 °C/min up to 600 °C. Data were collected during this heating period.

Fourier Transform Infrared Absorption Spectroscopy (FT-IR). Fourier transform infrared spectroscopy (FT-IR) was performed on a Nicolet 520 FTIR spectrometer equipped with a 1 mW He−Ne laser. All spectra were obtained at room temperature under a nitrogen atmosphere. Background spectra were collected immediately prior to the recording of sample spectra. Metal complexes dispersed within a KBr matrix were hand-pressed into transparent disks and vacuum-dried at room temperature for 24 h prior to data collection. Spectra were averaged from 60 scans.

Fourier Transform Laser Raman Spectroscopy (FT-LRS). FT-Raman scattering data was collected at the Hong Kong University of Science and Technology using standard spectroscopic techniques. Samples were exposed to the laser beam as KBr pellets consisting of approximately 1 mg sample per 300 mg of KBr. Data were acquired on a Bruker IFS 66 FT-Raman/FT-IR instrument equipped with a highly sensitive, liquid nitrogen cooled GE diode detector. Spectra were recorded via 180° scattering. A 1.064 μm laser excitation was used to collect 3000 scans per sample. The laser power was 300 mW (output).

Atomic Force Microscopy (AFM). The AFM used for these experiments was a contact mode microscope from Digital Instruments calibrated by imaging mica. Pillared montmorillonite samples were pressed at 10 000 lbs into wafers that were then glued with an epoxy resin onto steel disks. After the glue dried, the AFM tip was carefully placed in the middle of the wafer. The images reported contain either 200 × 100 or 256 × 256 data points and nearly all images were acquired within seconds. The Si_3N_4 cantilevers (with integral tips) used for imaging were 120 μm in length and possessed a spring constant of 0.6 N/m. The force applied was in the 10−100 nN range. The utility of AFM to characterize clays[39,40] and the Digital Instrument microscope used in this research have been discussed elsewhere.[41]

X-ray Photoelectron Spectroscopy (XPS). A Leybold-Hereaus LHX-11 X-ray photoelectron spectrometer was used to examine the precursor and Co-containing pillared clays in their as-prepared forms. Powder samples were formed into thin, self-supporting wafers with a hydraulic press and pellet die. Approximately 0.02 g of the sample was placed in the die and pressed under approximately 35 MN/m^2 of pressure. The wafer thus formed was mounted on the XPS sample holder and inserted into the spectrometer. The Mg X-ray source was operated at 250 W power, with spectra collected as a function of time of X-ray irradiation at a constant pass energy of 100. After the computer-controlled acquisition, spectra were examined for intensities and peak positions using a nonlinear background subtraction and the sensitivity factors for the spectrometer. The binding energies of all peaks were referenced to the ubiquitous C1s peak at 284.6 eV.

Results

Elemental Analysis. Co_3−PILC composition data show N/Co molar ratios that are slightly higher than those predicted by theory, which may be due to some solvent occlusion (Table 2). Higher C/Co values have been attributed to carbon impurities in the parent Na−montmorillonite. Elemental analyses for chlorine have indicated that perchlorate impurities are not present in any measurable amount in the samples tested.

Pillared Ca−montmorillonite, which has no intrinsic carbon, and pillared Laponite, which possesses very little, exhibit C/Co molar ratios approaching those predicted by theory. This result is consistent with the

(37) Gerasenkova, A. N.; Udovenko, V. V. *Russ. J. Inorg. Chem*. **1968**, *13*, *11*, 1551.
(38) Evreev, V. N. *Russ. J. Inorg. Chem*. **1967**, 12, 8, 1112.
(39) Hartman, H.; Sposito, G.; Yang, A.; Manne, S.; Gould, S. A. C.; Hansma, P. *Clays Clay Miner*. **1990**, *38*, 33.
(40) Lindgreen, H.; Garnaes, H.; Hansen, P. L.; Basenbacher, F.; Laegsgaard, E.; Steinsgaard, I.; Gould, S.; Hansma P. *Am. Miner*. **1991**, *76*, 1218.
(41) Occelli, M. L.; Drake, B.; Gould, S. *J. Cat*. **1993**, *142*, 337.

Table 2. Elemental Analyses for Trimer-Pillared Smectites

	% Co	% C[b]	% N	C/Co	N/Co	C/N
$Co_3(eta)_6(ClO4)_3$[a]	21.15	17.25	10.06	4.0	2.0	2.0
1 bentolite H	0	0.77	0			
2 ST-Co-S3-A	3.8	4.7	2.0	6.0	2.2	2.7
3 ST-Co-S3-B	2.5	3.9	1.3	7.0	2.0	3.5
4 ST-Co-S3-C	1.5	2.5	.86	8.2	2.3	3.4
5 ST-Co-S3-D	0.89	2.0	.5	11.0	2.3	4.6
6 ST-Co-S3-E	2.7					
7 ST-Co-S3-F	1.6					
8 ST-Co-S3-G	0.96					
9 bentolite L	0	0	0			
10 ST-Co-S4	4.3	4.0	1.7	4.6	1.7	2.7
11 hectorite	0	6.2	0			
12 ST-Co-S5	3.3	8.2	1.2	12.2	1.5	7.9
13 Laponite	0	.20	0			
14 ST-Co-S6	3.8	3.6	1.6	4.5	1.8	2.5
15 saponite	0	.22	0			
16 ST-Co-S7	3.6	4.1	1.5	5.6	1.8	3.1

[a] eta = diprotonated aminoethanol. [b] C values include C impurities in the parent clay.

presence of the trimeric cation in the clay interlamellar space. The absolute loading of the pristine trimeric cation (M_w= 537) may be determined from elemental analysis of the samples; results are summarized in Table 2. In a Ca−montmorillonite containing 3.8% Co, there are 0.115 g of trimer/g of PILC (or 0.642 mequiv of trimer/g of PILC). Knowing that there are 0.885 g of clay/g of PILC, this Co_3−PILC sample contains therefore 0.726 mequiv of trimer/g of clay. This result is in agreement with the montmorillonite average cation exchange capacity (CEC) of approximately 0.80 mequiv/g of clay.[1] The pillared Na−montmorillonite containing 4.3% Co has exceeded this value (Table 2). In either case, it appears that the interlayer space of the clay is saturated with pillars.

The presence of excess intercalant on the clay surface has been observed both by AFM and XRD. Furthermore, XPS results (vida infra) indicate that the trivalent Co trimer is reduced to its divalent analogue during the pillaring reaction. As a result, CEC values will be larger than those calculated by assuming a trivalent pillar charge. Exchange of cations beyond the clay's CEC has been observed in other pillared materials.[42−44] In the clay samples under study, Co trimer loading increases with increasing layer charge and with trimer/Na−montmorillonite ratios used during synthesis. However, the relationship is not linear. In Figure 2, the slope for the experimental uptake of the trimeric complex is not constant, suggesting that different pillaring processes are occurring as the trimer/clay ratio changes during synthesis. The smaller trimer uptake at lower trimer/clay ratios may be due to trimer adsorption on the clay exterior or to the exchanging of interlamellar cations near the layer edges. The increased uptake at higher trimer concentrations suggests that cooperative diffusion is now occurring. That is, Co trimers, acting as wedges, increase expansion of the clay layers and expose regions previously inaccessible to ion exchange.

Solvent effects on pillared clays compositions have been investigated only for montmorillonite samples;

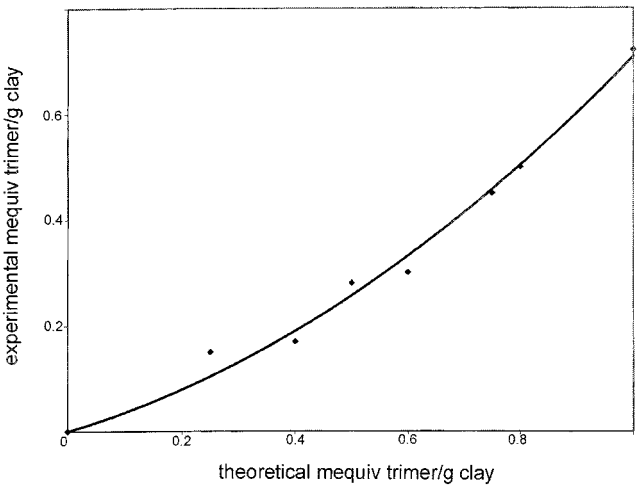

Figure 2. Uptake of $[Co_3(OC_2H_4NH_2)_6]^{3+}$ ions during the pillaring of Ca−montmorillonite (Bentolite-H).

Table 3. Elemental Analysis Data for Several PILCs[a]

pillar/solvent	% Co	% C	% N	C/Co	N/Co	C/N
$[Co_3(eta)_6](ClO_4)_3$/MeOH	2.47	2.94	1.21	5.84	2.06	2.83
$[Co_3(eta)_6](ClO_4)_3/H_2O$	4.25	1.92	0.94	2.21	0.93	2.37
$[Co_3(eta)_6](Ac)_2$/MeCN	3.92	4.11	1.78	5.14	1.91	2.69
$[Co_2(eta)_3(etaH)_3](NO_3)$[b]	2.94	4.23	1.73	7.06	2.48	2.85
$[Co(eta)_3]\cdot 3H_2O$/MeCN	3.79	4.90	2.08	6.34	2.31	2.74

[a] Elemental ratios are mol/mol. C data is not corrected for the parent clay C impurities. eta = deprotonated 2-aminoethanol. Ac = acetate. [b] Sample prepared in a 10:1 acetonitrile/methanol mixed solvent system.

results are given in Table 3. The N/Co molar ratio for the Co_3−PILC prepared in methanol matches the value theoretically predicted for the Co trimer. As with samples prepared in acetonitrile, the inflated C/N and C/Co ratios in Table 3 are attributed to carbon impurities in the parent clay and to some solvent occlusion, respectively. The 2.47% Co loading is somewhat lower than the 2.70% Co observed in Table 2 for a sample prepared in ACN with the same Co complex/clay ratio.

Co_3−PILC samples prepared in water have C/Co and C/N molar ratios consistent with a ligand:cobalt ratio of 1:1, indicating that the tris chelate is decomposed. In fact, the powder XRD spectrum (not shown), exhibits a *d* spacing too small to accommodate the pristine trimeric cation. The decomposition of the trimer is not unexpected because of its limited stability in water. The metal loading is higher than in trimer-pillared samples prepared in ACN. This result has been attributed the reduction of the cobalt to a +2 oxidation state, which is believed to occur upon ligand loss.

In samples pillared with $[Co_3(OC_2H_4NH_2)_6](CH_3CO_2)_2$, N/Co molar ratios are consistent with the presence of $[Co_3(OC_2H_4NH_2)_6]^{2+}$ in its pristine form. Data in Table 3 indicate that, in agreement with the intercalant's lower charge, the sample contains more cobalt (3.92%) than any of the clays pillared with $[Co_3(OCH_2CH_2NH_2)_6]^{3+}$ in ACN. The C/N molar ratio (2.70) is close to that observed in samples pillared with the trivalent cobalt trimer, confirming that no significant ethylene glycol (the wedging agent employed) residue is present in the pillared product.

Montmorillonites expanded with the cobalt monomer $[Co(OC_2H_4NH_2)_3]\cdot 3H_2O$ or with the dimer $[Co_2(OC_2H_4NH_2)_3(HOC_2H_4NH_2)_3](NO_3)_3$ should give identical theo-

(42) Barrer, R. M.; Brummer, K. *Trans. Faraday Soc.* **1963**, *59*, 959.
(43) Theng, B. K.; Grenland, D. J.; Ouirk, J. P. *Clay Miner.* **1967**, *7*, 1.
(44) Giannelis, M.; Karrado, K. *Chem. Mater.* **1990**, *2*, 328.

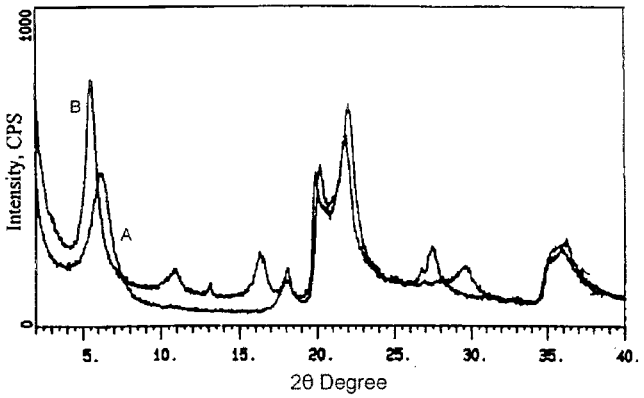

Figure 3. Powder XRD pattern of Na−montmorillonite (A) before and (B) after pillaring with $[Co_3(OC_2H_4NH_2)_6]^{3+}$ ions (the PILC contains 4.4% Co).

retical molar ratios. In Table 3, the measured N/Co ratios are 2.31 and 2.48, that is, lower than the expected value of 3.0 for the monomer and dimer PILC. This discrepancy has been attributed to the partial decomposition of the complexes during pillaring. Ethylene glycol was used as a wedging agent in the synthesis of the monomer−PILC sample. Its C/N ratio (2.74) is similar to that observed for cobalt-pillared montmorillonites in ACN, indicating the absence of occluded ethylene glycol. In Table 3, C/Co molar ratios are greater than the expected value of 6.0 because of carbon impurities in the parent clay. In conclusion, a solution of the Co trimer in ACN is the best pillaring agent to expand the clay samples under study.

Powder XRD Results. *Montmorillonites.* As mentioned above, Na−montmorillonites, when allowed to react with $[Co_3(OCH_2CH_2NH_2)_6]^{3+}$ ions in ACN, undergo an expansion that depends on Co loading (Figure 3). The parent clay has a *d* spacing of 1.26 nm and a 0.03 nm interlayer expansion caused by occluded ACN. Initially, when the complex loading is only 0.15 mequiv/g of clay, the interlamellar spacing expands to 0.49 nm, a dimension consistent with the trimeric cation approximate width of 0.48 nm; see Figure 3. Thus, given the room to do so, the Co trimer preferentially adopts an orientation parallel to the montmorillonite surface. This is surprising because in this position the cation can only interact with the basal oxygens that form the silicate layers, through the C−H bonds of the amminoethanol ligand. The greater polarity of the N−H bonds would predict that ligand nitrogens should be the preferred bonding sites. Initially, at these low Co trimer concentrations, NH_2 groups do not appear to influence pillar orientation.

When the complex loading is increased to 0.17 mequiv/g of clay, the Co_3−PILC *d* spacing increases to 0.52 nm. Since the trimeric cation length is 0.72 nm, pillars now lies at a 46° angle relative to the montmorillonite interlayer surface. The increase in pillar density appears to force the cations to adopt a more upright position. For trimer loadings in the 0.28−0.50 mequiv/g of clay range, the interlamellar height remains between 0.54 and 0.55 nm, implying that the surface-to-pillar angle is now between 48.6° and 50° (Figure 3).

After increasing the trimer loading to 0.72 mequiv, the clay interlamellar expansion increases to 0.67 nm and the surface-to-pillar angle to 68°; see Figure 4. The increase in *d* spacing is attributed, in part, to the

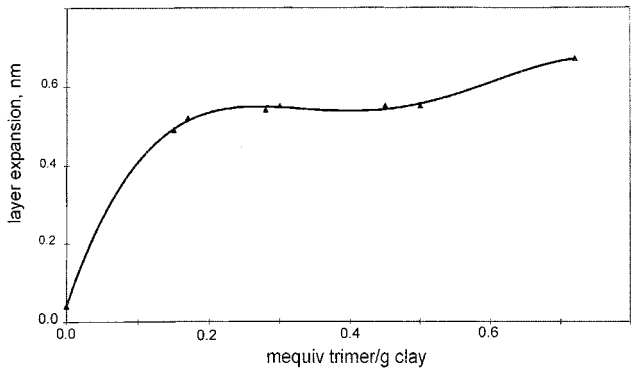

Figure 4. Changes in the clay interlayer expansion with $[Co_3(OC_2H_4NH_2)_6]^{3+}$ ions loading.

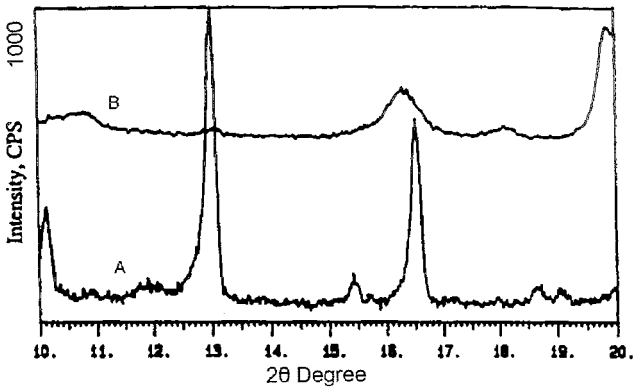

Figure 5. Powder XRD pattern of (A) the $Co_3(H_2NCH_2CH_2O)_6(ClO_4)_3$ salt and (B) Ca−montmorillonite pillared with $[Co_3(OC_2H_4NH_2)_6]^{3+}$ ions (the PILC sample contains 3.8 wt % Co).

clustering of the trimeric pillars within the interlamellar space. This alteration in pillar orientation with pillar density has been noted in other pillared clay systems containing alkylammonium cations (some with long organic chains) or porphyrins capable of different orientations.[42−44] The aggregation of organometallic complex pillars as a function of the pillar charge/clay charge ratio in montmorillonites has been discussed elsewhere.[45]

The XRD diffractogram of the Co_3−PILC with the heaviest metal loading (3.8% Co) contains several diffraction lines between 10° and 20° which cannot be attributed to the parent clay (Figure 4). Comparison of the PILC diffraction pattern with that of the trimeric cobalt salt allows some correlation between diffraction lines (Figure 5). The peak at 16.6° appears in both the complex and the Co_3−PILC pattern. However, the more intense peak at 12.9° in the complex diffractogram does not appear in the pillared product pattern.

After expanding Ca−montmorillonite with $[Co_3(H_2NCH_2CH_2O)_6](ClO_4)_3$ in ACN, the *d*(001) reflection of the Co_3−PILC indicates a basal spacing of 1.58 nm, representing an interlamellar expansion of 0.62 nm. Although it has a higher metal loading (0.84 mequiv/g of clay), this expansion is less than the one (0.67 nm) seen in its Na counterpart. Elemental analysis data have indicated that pillared Na− and Ca−montmorillonites contain one cobalt trimer for every 5.7 unit cells and one cobalt trimer for every 2.7 unit cells of clay, respectively. The decreased pillars density may limit

(45) Tsvetkov, F.; White, J. *J. Am Chem. Soc.* **1988**, *110*, 3183.

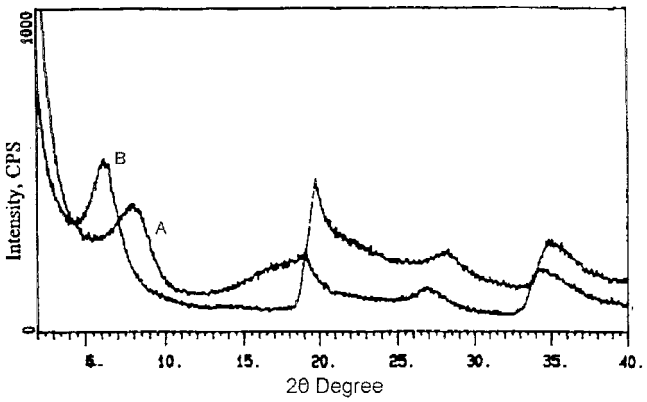

Figure 6. Powder XRD pattern of saponite (A) before and (B) after pillaring with $[Co_3(OC_2H_4NH_2)_6]^{3+}$ ions (the PILC material contains 3.6 wt % Co).

pillar aggregation[8] and cause a smaller expansion of the Ca−bentonite layers. The cobalt loadings of 0.84 mequiv of trimer/g of clay exceed the clay cation exchange capacity because of crystallite formation (seen by XRD), trimer deposition on the exterior surface of the clay (seen by AFM), and reduction of Co(III) to Co(II) as observed by XPS.

Other Clays. Hectorite, when pillared with $[Co_3(H_2NCH_2CH_2O)_6](ClO_4)_3$ in ACN, exhibits an increase in interlayer spacing from 0.32 to 0.57 nm. This spacing is less than that observed for either pillared montmorillonite sample, though its layer charge density is similar to that of Na−montmorillonite (Table 1). No spectral evidence of crystallite formation was observed.

Reaction of Laponite with $[Co_3(H_2NCH_2CH_2O)_6](ClO_4)_3$ in ACN generates a pillared product containing 0.73 mequiv of trimer/g of clay. Its XRD diffractogram (not shown) does not contain evidence of crystallite formation. It is characterized by a *d*(001) peak at 1.60 nm implying an interlamellar expansion of 0.64 nm. Laponite differs from the other clays in that more than half of the surface hydroxyls have been replaced with fluoride anions. This substitution appears to result in a variety of pillar orientations and to generate a *d*(001) reflection broader than those seen in montmorillonite samples. Similar results have been observed when reacting Laponite with large quaternary ammonium cations.[46] Saponite, the clay sample with the lowest layer charge, reacts with $[Co_3(H_2NCH_2CH_2O)_6](ClO_4)_3$ in ACN to yield a pillared product containing the lowest (0.69 mequiv/g of clay) trimer amounts. Its XRD pattern exhibits a *d*(001) basal spacing of 1.44 nm, indicating a pillar orientation parallel to the clay surface (Figure 6). Saponite and Laponite possess some isomorphous substitution in their tetrahedral layers. The layer charge is generally believed to be more homogeneous and centered in tetrahedrally rather than in octahedrally substituted clays. Studies by Wear[47] and Weaver[48] have concluded that removal of the interlamellar ion is more difficult when the matrix charge has a tetrahedral rather than octahedral origin, explaining in part the lower Co loading in the pillared saponite sample**.** This charge density distribution may also be influencing pillar orientation. Elemental analysis of these pillared clays can be found in Table 2. The effects of other solvents on PILC preparation is described below.

Solvent Effects. The $[Co_3(H_2NCH_2CH_2O)_6](ClO_4)_3$ and Na−montmorillonite reaction in methanol yields a pillared sample with basal spacing of 1.43 nm, corresponding to a pillar orientation parallel to the clay surface. However, the possibility of complex decomposition to the neutral cobalt monomer $[Co(H_2NCH_2CH_2O)_3]$ and to the aquated cation $[Co(OH_2)_6]^{2+}$ after intercalation cannot be excluded. The Co monomeric species is very stable, and the *d* spacing observed is precisely that predicted for a monolayer of the cobalt monomer occupying the interlayer region.

Similar results are obtained when the pillaring reaction is performed in water. In this case, the metal loading is high (4.6%) and crystallite formation is not observed. As before, a 1.41 nm *d* spacing is consistent with the dimensions of the aquated cation $[Co(H_2O)_6]^{3+}$. This decomposition of the complex cation in water is not wholly unexpected. In fact, UV−vis spectra of the trimer refluxed in distilled water (not shown) indicate complete decomposition of the complex after 96 h.[36] The preparation of PILC containing other Co complexes is discussed below.

Effects of Co Complexes. Interactions of the divalent trimer $[Co_3(H_2NCH_2CH_2O)_6](CH_3CO_2)_2$ with Na−montmorillonite in ACN are somewhat different. The pillaring agent in this material is isostructural with the trimeric cobalt cation used to pillar earlier samples, but the cationic charge is reduced to +2 due to the lower valency of the central cobalt. The pillared product has a *d* spacing of 1.59 nm, corresponding to an interlayer distance of 0.63 nm. Although this is a higher (0.74 mequiv/g of clay) complex loading than any of the Na−montmorillonites pillared with the trivalent cation, the reduction in charge of Co trimer appears to induce the pillar to orient at an angle of 61°, that is, nearer to the clay surface.

The dimeric cobalt cation $[Co_2(H_2NCH_2CH_2O)_3(H_2NCH_2CH_2OH)_3](NO_3)_3$ intercalated in the Na−montmorillonite exhibits a *d*(001) peak corresponding to a 0.47 nm interlayer spacing, which is too small to accommodate the pristine cation in the interlamellar region. Elemental analysis in Table 3 supports this conclusion. The interlayer expansion is identical to the one predicted for a monolayer of $[Co(H_2NCH_2CH_2O)_3]$ trischelate. Though this is a probable decomposition product, elemental analysis data give a ligand:metal ratio of 2.5:1, inconsistent with the presence of the pristine $[Co(H_2NCH_2CH_2O)_3]$ complex. Furthermore, the C/Co molar ratio is lower than predicted by theory, indicating that ligand losses from the monomer have occurred.

The powder XRD of Na−montmorillonite pillared with the neutral cobalt monomer $[Co(H_2NCH_2CH_2O)_3]\cdot 5H_2O$ (not shown) displays a basal spacing larger (1.55 nm) than expected. An interlamellar distance of 0.59 nm is too large to represent a single layer of pillars and could indicate the presence of occluded ethylene glycol. Ligand/cobalt molar ratios of 2.3/1 suggest that some decomposition of the cobalt pillars has occurred. The *d* spacing does not correspond to the Co monomer dimen-

(46) Occelli, M. L.; Iyer, P. S.; Sanders, J. V. In *Zeolites: Fact, Figures and Future*; Proc. 8th. IZA Mtg.; Elsevier: New York, 1989; Part A, p 1311.
(47) Wear, J. I.; White, J. L. *Soil Sci.* **1951**, *71*, 1.
(48) Weaver, C. E. *Am. Miner.* **1958**, *43*: 839.

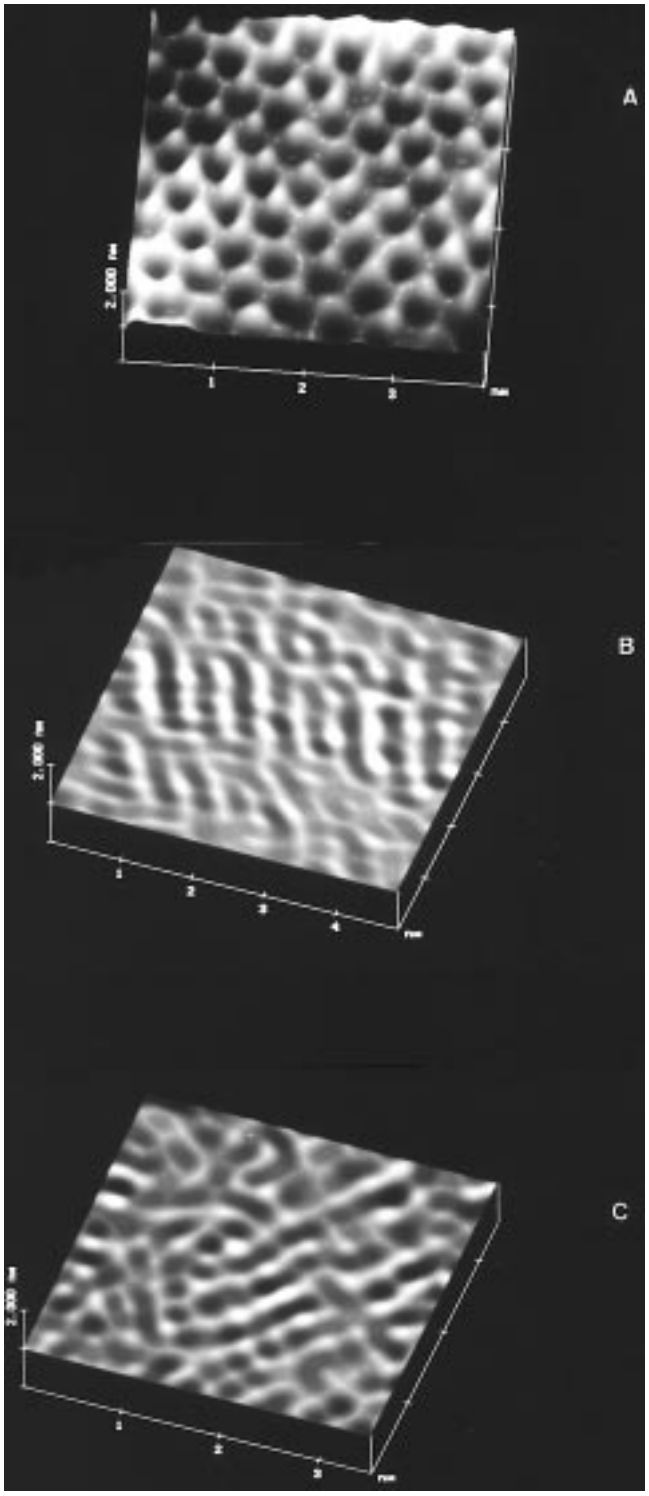

Figure 7. Atomic scale images of the parent montmorillonite surface (A) before pillaring, (B) after pillaring with $[Co_3(OC_2H_4NH_2)_6]^{3+}$ ions, and (C) variation of the image in B with time.

sions, probably because different Co species are present in the clay interlamellar region.

AFM Results. AFM images were obtained to ascertain the presence (or absence) of pillaring agents on the clay surface. AFM images of the parent Texas montmorillonite consist of a collection of bright spots in a well-ordered hexagonal pattern with distances between nearest and lateral neighbors at 0.52 and 0.90 nm, respectively[39−41] (Figure 7A). These results are in agreement with the geometry of the basal plane of 2:1 clay minerals.[1] Images of the external surface of the PILC did not exhibit the expected repeat distances of the parent clay SiO_4 oxygens, owing to the presence of trimer ions on the clay's external surface (Figure 7B). Limited regions of ordered rows of white spots 0.32 nm in width forming clusters of three white spots with an average length of 0.74 nm were observed (Figure 7B). These dimension are consistent with those (0.72 nm × 0.41 nm) of the Co trimer. The distance between the rows was 0.51−0.53 nm.

Table 4. TGA Results for the Trimer-Pillared Na−Montmorillonite in ACN[a]

	ligand loss			
sample	theory	exptl	loss ratio	%Co
ST-Co-S3-A	7.8%	250−350 °C, 2.01% 350−450 °C, 6.01%	1:3.0	3.8
ST-Co-S3-B	5.0%	250−350 °C, 1.07% 350−475 °C, 3.96%	1:3.9	2.5
ST-Co-S3-C	3.2%	250−350 °C, 1.19% 350−475 °C, 2.26%	1:1.9	1.5
ST-Co-S3-D	1.8%	250−325 °C, 0.76% 325−450 °C, 0.99%	1:1.3	0.89

[a] Experimental mass losses have been corrected for those of the parent clay. Loss ratio is the (second ligand mass loss)/(first ligand mass loss) ratio.

The parameters of the inorganic complex suggest that the molecule is laying on its side, probably bonding through one or more of its ═N−H groups. Bonding through the ligand oxygens is possible, but unlikely, because the cationic trimer is expected to selectively bond to the anionic surface sites.

As the imaging session progressed, the surface topography changed completely (Figure 7C). The tip of the cantiliver acts as a molecular broom rearranging the surface distribution of trimer molecules. Thus, the trimer−clay surface interactions are similar to those between amines and zeolites but weaker then those observed between quaternary ammonium cations and zeolites.[49] In summary, in agreement with XRD results, AFM images indicate that the expanded clay surface contains an adsorbed species whose dimensions are consistent with those of the Co trimer.

Thermogravimetric Analysis Results. The derivative thermogravimetric profile for the decomposition in air of all four cobalt PILCs prepared with $[Co_3(H_2NCH_2CH_2O)_6](ClO_4)_3$ in ACN are qualitatively similar (Table 4). For the Co_3−PILC samples described in Table 2, mass losses in the 250−350 and 350−450 °C temperature range agree with the expected theoretical losses from the ligands; see Table 4. Thermal decomposition of the similar salt $[Co_3(H_2NCH_2CH_2O)_6](CH_3CO_2)_2$ in air shows that ligand decomposition occurs at lower temperatures than in its pillared samples. Furthermore, the ratio between the two ligand mass losses suffered by the Co complex changes significantly before and after intercalation. The increased thermal stability of the Co cation has been attributed to its ligands interaction with the clay silicate layers. In addition, none of the Co/C ratios correspond to an integral split between the trivalent Co cations six ligands, indicating that some trivalent and divalent Co complexes could be present.

(49) Weisenhorn,, J. E.; MacDougal, J. E.; Gould, S. A. C.; Cox, D. S.; Wise, W. S.; Maivold, P.; Elings, V. B.; Hansma, P. K.; Stucky, G. D. *Science* 1990, *247*, 1330.

The third mass loss is attributed to the dehydroxylation of the clay silicate layers. For the Co_3−PILC sample containing 3.8% Co, the *d* spacing decreases from 1.62 to 1.43 nm in the 100 and 250 °C temperature range because of solvent losses or reorientation of the Co pillars within the interlamellar region (Table 4). Between 250 and 350 °C, the first loss of ligand mass occurs, causing the interlayer spacing to decrease only by 0.015 nm. Thus the lost ligands are not directly involved in bonding the pillars with the interlamellar space. Above 350 °C the *d* spacing drops sharply and evidence of a pillared structure disappears, indicating that the second mass loss involves ligands interacting with the clay surface.

Different results have been observed when using methanol or water as the solvent. In fact, clays pillared using methanol solutions of the $[Co_3(H_2NCH_2CH_2O)_6](ClO_4)_3$ salt exhibit a mass loss of 1.77 wt % in the 100−280 °C temperature range followed by a 4.15 wt % loss between 280 and 450 °C. A final weight loss of 2.46 wt % occur between 450 and 500 °C. The expected mass loss for a CoO residue is 4.36%; a Co_3O_4 residue would result in a 4.13 wt % loss. (Co_3O_4 begins to form near 400 °C and the calcination residue is probably a Co_3O_4−CoO mixture.). The cumulative loss from 100 to 450 °C is larger (5.91 w %) than expected. The parent clay exhibits a loss of 1.7 wt %/g of clay (or a 1.6%/g of PILC) over the aforementioned temperature region. Thus the observed mass loss which may be attributed to the ligands is 4.31 wt %, suggesting that most of the Co is present as a CoO residue. The clay environment appears to inhibit Co_3O_4 formation. In agreement with DTA results, TGA of the Co_3−PILC prepared in methanol (and containing 2.47% Co) indicates that initial ligand loss occurs at much lower temperature then observed for samples prepared in ACN. XRD results indicate a pillar orientation similar to that of a Co_3−PILC containing 0.89% Co and prepared in ACN. The lower thermal stability for the Co_3−PILC prepared in methanol is attributed to weaker pillar interactions with the clay's silicate layers.

Similarly, when $Co_2(H_2NCH_2CH_2O)_3(H_2NCH_2CH_2OH)_3](NO_3)_3$ is used as the pillaring agent, the Co_2−PILC displays three distinct regions of weight loss. It loses 2.42%, 5.77%, and 2.64% in the 100−310, 310−470, and 470−600 °C temperature range, respectively. The Co_2−PILC cumulative mass loss at 470 °C accounts only for 84 wt % of the total ligand mass loss predicted by theory, indicating that (in agreement with elemental analysis data) partial ligand loss occurs during the pillaring process. After correcting for the 3.0 wt % loss attributable to the clay support, the total loss is calculated to be 7.82 wt %, well in agreement with a 7.92% weight loss associated with a Co_3O_4 residue formation.

Na−montmorillonite pillared with the cobalt monomer $Co(H_2NCH_2CH_2O)_3 \cdot 3H_2O$ displays three regions of mass loss. A 2.47 wt % decrease occurs between 100 and 290 °C, followed by a second, larger loss of 7.28 wt % between 290 and 477 °C. The final decrease of 2.38 wt % occurs between 477 and 600 °C. Assuming a Co_3O_4 calcination residue, the total theoretical weight loss attributed to the ligands would be 10.2%. The actual loss observed is 9.36%, suggesting that the Co complex loses some of its ligand during the pillaring reaction.

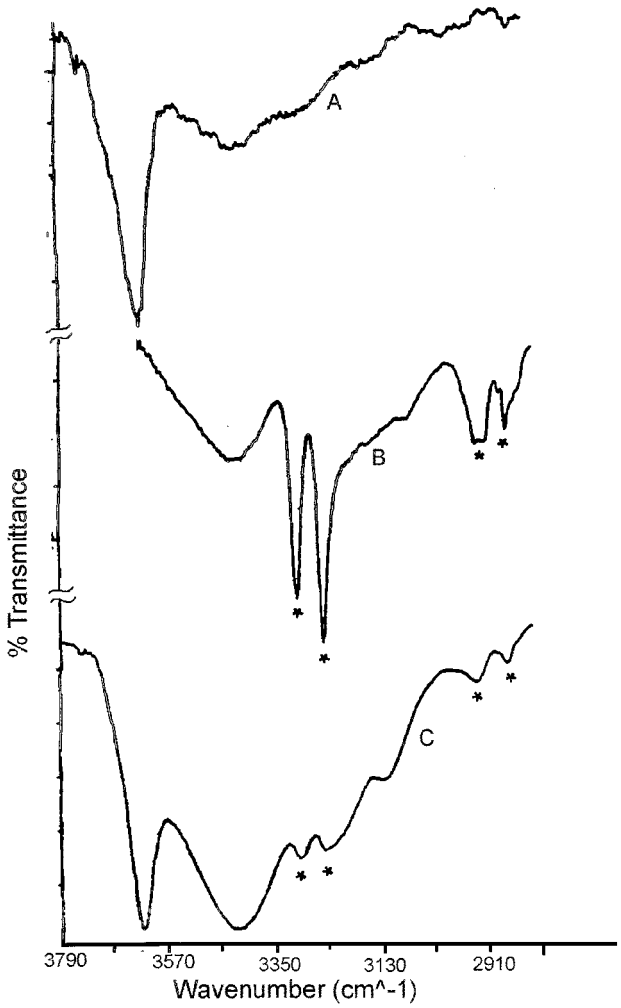

Figure 8. Transmittance FTIR spectra of (A) the parent Ca−montmorillonite, (B) the $Co_3(H_2NCH_2CH_2O)_6(ClO_4)_3$ salt, and (C) Ca−montmorillonite pillared with $[Co_3(OC_2H_4NH_2)_6]^{3+}$ ions (sample 2, Table 2).

FT IR Results. FT IR studies have been limited to pillared montmorillonite samples. Results have shown that all the four reference clay samples exhibit broad bands near 3400 cm^{-1} which can be attributed to an O−H stretch either from water or from the protonated ligand. The sharp band at 3645 cm^{-1} can be attributed to the free OH symmetric stretch of the silanol groups associated with the clay silicate layers (Figure 8A).

Solution-state ethanolamine normally exhibits symmetric and asymmetric NH_2 stretches at 3452 and 3230 cm^{-1}, respectively. The intensity of the symmetric stretch is normally 98% that of the asymmetric stretch, but this ratio may change in case of asymmetric bonding of the hydrogens. Salts such as $[Co_3(H_2NCH_2CH_2O)_6](ClO_4)_3$ display intense bands of this nature at 3308 and 3255 cm^{-1} (Figure 8B). In the divalent trimer, these bands are shifted to 3237 and 3099 cm^{-1} (lower frequencies). Bands are somewhat broader than those in the spectrum of the trivalent complex, thus making frequency assignment more difficult. In the dimeric Co complex, $-NH_2$ stretching bands are at 3275 and 3139 cm^{-1}; the symmetric stretch is nearly masked by a NH deformation overtone frequency at 3225 cm^{-1}. The monomer exhibits broad NH_2 peaks at 3194 and 3119

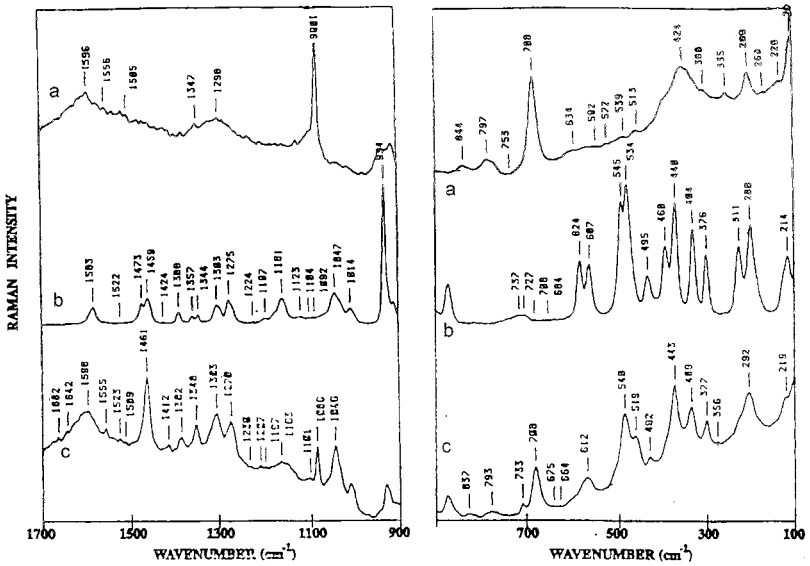

Figure 9. FT-Raman spectra of (A) the parent Ca−montmorillonite, (B) the $Co_3(H_2NCH_2CH_2O)_6(ClO_4)_3$ salt, and (C) Ca−montmorillonite pillared with $[Co_3(OC_2H_4NH_2)_6]^{3+}$ ions (sample 2, Table 2).

cm^{-1}, but these are less intense than those of other cobalt species. These Co complexes exhibit bands near 2930 and 2879 cm^{-1}, assigned to ligand methylene groups.[50]

Na−montmorillonite pillared with $Co_3(H_2NCH_2CH_2O)_6(ClO_4)_3$ (in ACN) exhibits stretches in the 2800−3800 cm^{-1} infrared region containing frequencies of both the trimeric salt and of the parent clay (Figure 8C). The broader hydrogen-bonded OH absorption near 3400 cm^{-1} is observed in both the clay and Co trimer. In the Co_3−PILC, the NH_2 symmetric and asymmetric stretch of the trimeric cation at 3308 and 3255 cm^{-1} can be seen at 3305 and 3254 cm^{-1}. The NH bands are of particular interest because they are absent in the parent clays. The ligand nitrogens are a possible source for bonding with the basal oxygens that form the clay silicate layers. Therefore changes in the intensity, shape, and position of these bands may be correlated with the nature of the interactions between the pillaring agents and the clay interlamellar space.

Bands in Figure 8C are broader than in the cobalt salt spectrum in Figure 8B, suggesting some variation in environment for the ligand nitrogens after pillaring. This is confirmed by the change in the intensity ratio between the two NH_2 bands. The asymmetric NH_2 stretch is normally 2% more intense than its symmetric counterpart. However, the Co_3−PILC sample exhibits an asymmetric resonance which is 98% of the symmetric stretch intensity. The shift in intensity ratio from the salt to the Co_3−PILC is attributed to asymmetric bonding of the amine hydrogens with the basal oxygens of the clay silicate layers. Asymmetric and symmetric $-CH_2$ stretches, observed at 2926 and 2881 cm^{-1} in the cobalt salt, are seen at 2942 and 2878 cm^{-1} in the Co−PILC. These peaks are still visible in the clay samples pillared with lower (<4%) Co loadings.

When using methanol as a solvent for $[Co_3(H_2NCH_2CH_2O)_6](ClO_4)_3$, the Co_3−PILC spectrum contains bands at 2930 and 2878 cm^{-1} (not shown), attributed to the asymmetric and symmetric CH_2 stretches of the ligand, but does not contain NH stretching modes of the trimeric cation seen in the spectrum of Co_3−PILCs prepared in ACN. Similarly, NH_2 stretching modes are not visible in the spectrum of Co_3−PILC prepared in water. This is expected as powder XRD and elemental analysis suggest that the trimeric cation is not stable in water. The CH_2 stretches at 2930 and 2879 cm^{-1} indicate the presence of some ligand, a result consistent with elemental data in Table 3, which indicates a ligand: cobalt ratio of 1:1 in this sample. Thus the environment of the ligand nitrogens in Co_3−PILC samples prepared in methanol is different from that of samples prepared in ACN.

FT-LRS Results. FT-LRS results for montmorillonites before and after pillaring with $[Co_3(H_2NCH_2CH_2O)_6]^{3+}$ in ACN are shown in Figure 9A,C. The FT-LRS spectrum of the $[Co_3(OCH_2CH_2NH_2)](ClO_4)_3$ salt is given in Figure 9B.[51] Particular attention was given to the nitrogen stretching modes in the 3200−3300 cm^{-1} region. The ν(N−H) modes of the complex were observed at 3260 and 3307 cm^{-1}. The ν(Co−N) mode appeared at 440 cm^{-1}. A sharp peak attributed to the perchlorate anion appeared at 935 cm^{-1}.[52] These frequencies were compared to those exhibited by a Co_3−PILC sample in Table 2 containing 3.8% Co, which possesses observable NH_2 bands.

The presence of the Co trimer in $[Co_3(H_2NCH_2CH_2O)_6]^{3+}$-expanded Na−montmorillonites (in ACN) can easily be confirmed by the peaks at 1461, 1382, 1348, 1303, 1270, 1163, 1046, 1012, 930, 875, 612, 540, 519, 492, 443, 409, 377, and 292 cm^{-1} in the Co_3−PILC Raman spectrum (Figure 9B,C). The parent clay bands in Figure 9A can be observed at 1596, 1086, and 708 cm^{-1}. The sloping baseline in the 1700−1100 and 650−200 cm^{-1} regions is also attributed to the parent montmorillonite. All the samples investigated have

(50) White, R. G. In *Handbook of Industrial Infrared Analysis*; Plenum Press: New York, 1978.

(51) Chopra, M.; Yu, N. T. Georgia Institute of Technology/Hong Kong; University of Science and Technology, personal communication, 1993.

(52) Kazuo, S. In *Infrared and Raman Spectra of Inorganic and Coordination Compounds*, 3rd ed.; J. Wiley and Sons: New York, 1978.

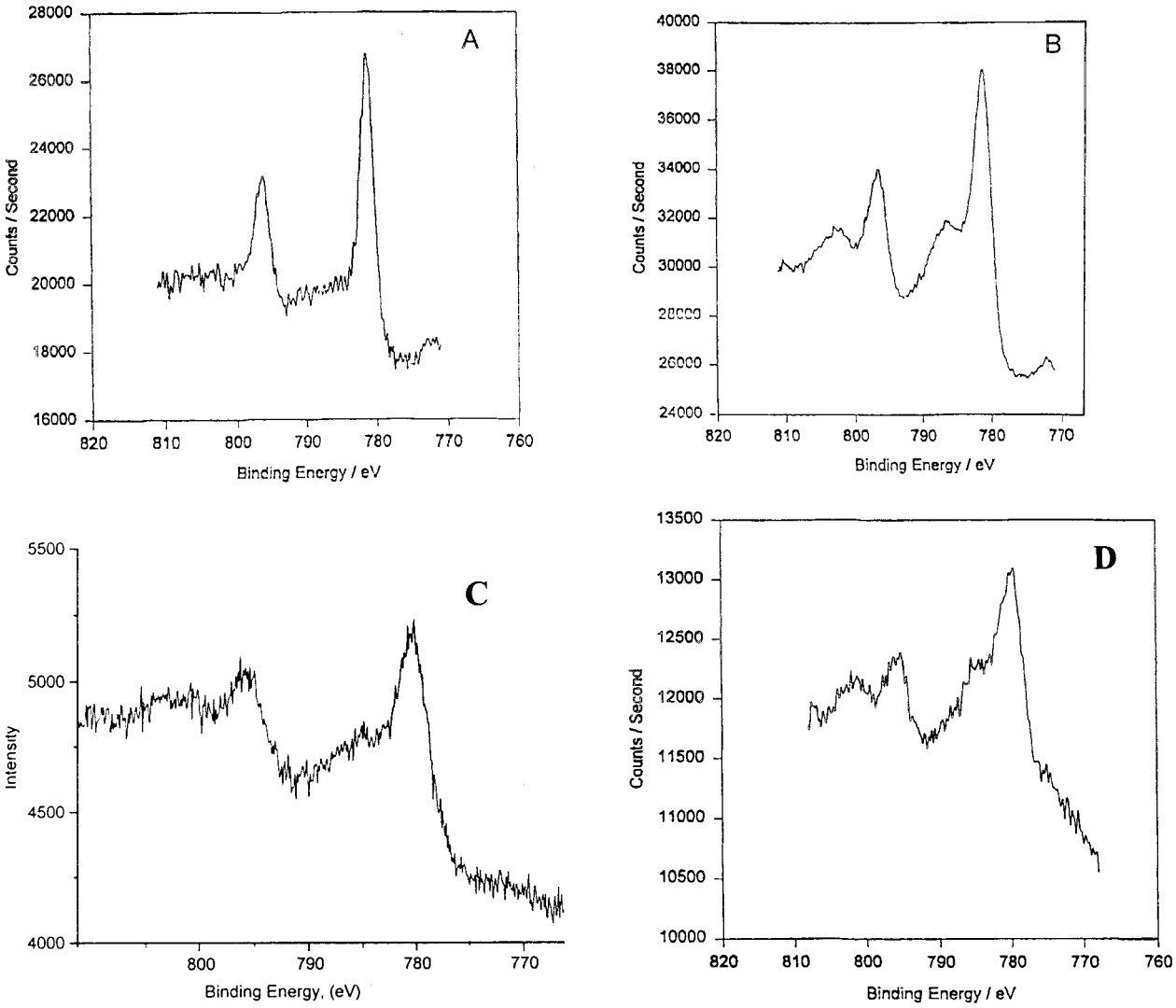

Figure 10. XPS spectra of the Co 2p region for the $Co_3(H_2NCH_2CH_2O)_6(ClO_4)_3$ salt after (A) 5 min and (B) 120 min. (C) The spectrum for the divalent $Co_3(H_2NCH_2CH_2O)_6(ClO_4)_2$ salt and (D) the spectrum for the Co_3−PILC sample.

corresponding peaks in the perchlorate salt spectrum, confirming that the pristine cation is indeed the pillaring agent initially responsible for the clay expansion.

XPS Results. The XPS spectra for the $Co_3(H_2NCH_2CH_2O)_6(ClO_4)_3$ salt, its divalent analogue $Co_3(H_2NCH_2CH_2O)_6(ClO_4)_2$, and the Co−PILC samples are displayed in Figure 10A−D. These spectra show the Co(III) trimer's sensitivity to X-ray irradiation, as is evidenced by changes in the intensities and positions of electron emission peaks as a function of time of data acquisition; see Figure 10A,B. As a consequence, spectra of the Co 2p region are presented to provide an indication of these changes and to ascertain the Co speciation after 5 min and after 2 h of evacuation and X-ray irradiation (Figure 10A,B). The positions of the Co peaks in the spectra of the Co salts are listed in Table 5. These data indicate the presence of Co(III) in the $Co_3(H_2NCH_2CH_2O)_6(ClO_4)_3$ salt with octahedral coordination.[53] After irradiation, as displayed in the 2 h collection data of Table 5, the intensity of the satellite peak at 785.2 eV for this Co(III) sample increased significantly.

Cobalt(II) ions produce strong satellite intensity, whereas Co(III) ions do not (Table 5). This structure has been assigned to a monopole charge transfer process (shake-up) from Co 2p → Co 3d and is characteristically stronger in cobalt(II) ions.[54] The separation between the satellite structure and the main Co $2p_{3/2}$ peak is normally near 5.0 eV for tetrahedrally coordinated cobalt(II) and near 6.0 eV for Co(II) in octahedral coordination. However, the spectrum of the divalent species, which is known to contain a central six-coordinate Co(II) in which the octahedron is severely elongated,[32,34] shows a separation of only 5.2 eV (Figure

Table 5. Positions of the Co 2p XPS Peaks in $Co_3(H_2NCH_2CH_2O)_6(ClO_4)_3$ and $Co_3(H_2NCH_2CH_2O)_6(ClO_4)_2$

	5 min collection	eV separation	120 min collection	eV separation
		Co(III) trimer		
Co $2p_{1/2}$	795.2		795.4	
Co $2p_{3/2}$	780.2	15.	780.0	15.4
satellite			785.2	5.2
		Co(II) trimer		
Co $2p_{1/2}$	795.6		796.1	
Co $2p_{3/2}$	780.2	15.4	780.2	15.9
satellite	785.2	5.0	785.3	5.1

(53) Chin, R. L.; Hercules, D. M. *J. Phys. Chem.* **1982**, *86*, 3079.

(54) Chuang, T. J.; Brundle, C. R.; Rice, D. W. *Surf. Sci.* **1976**, *59*, 413.

Table 6. Element Concentrations (in atom %) in the $Co_3(H_2NCH_2CH_2O)_6(ClO_4)_3$ and $Co_3(H_2NCH_2CH_2O)_6(ClO_4)_2$ Salts under Various Collection Conditions

element	Co(III) 5 min	Co(III) 120 min	Co(II) 5 min
Co	3.0	6.0	2.8
O	42.6	30.3	19.0
N	11.8	14.5	9.3
C	34.8	39.8	68.9
Cl	7.8	9.4	not measured

Table 7. Element Concentrations (in atom %) in Na−Montmorillonite Pillared with Solutions of the $Co_3(H_2NCH_2CH_2O)_6(ClO_4)_3$ Salt in ACN

element	Co	O	N	C	Si	Al
atom %	0.9	68.6	3.0	8.3	18.1	1.1

10C). The distortion of the octahedron is apparent from the values of the 12 O−Co−O angles that would be 90° angles if undistorted.[32] Six of these angles involve oxygens from the same shared face, and these average 76.4°, ranging from 75.7° to 76.7°; the other six involve oxygens from different shared faces and these average 103.6°, ranging from 102.2° to 105.6°.

In summary, extended periods of data collection under the conditions used can reduce the trivalent precursor to divalent species. In contrast, spectra of the $Co_3(H_2NCH_2CH_2O)_6(ClO_4)_2$ salt do not appear to be as sensitive to irradiation. Furthermore, the separation of the $2p_{3/2}$ and $2p_{1/2}$ peaks in the Co(II) trimer increases with time, changing from 15.4 to 15.9 eV. This increase is consistent with the presence of a octahedrally coordinated Co(II) species in the divalent Co trimer.

Elemental concentrations in the salt are presented in Table 6. The intensity of the Co 2p peak experienced the largest change in intensity. This change coincided with the reduction of Co(III) to Co(II). Also observed to change was the concentration of Cl together with the chemical form of the Cl. With a minimum amount of X-ray irradiation, at least three forms of Cl were observed, the electron peak positions of which indicate a speciation predominately $(ClO_4)^-$ but with some $(ClO_3)^-$ and chloride. With extended exposure, the intensity of the chloride peak increased while the intensity of the chlorate/chlorite peak decreased. The position of the N peak in the precursor suggests an organically associated element, as depicted in the precursor formula.

A spectrum of the Co 2p peak in the $[Co_3(OC_2H_4NH_2)_6]^{3+}$-pillared clay in ACN is presented in Figure 10D. Elemental concentrations are listed in Table 7. As in the divalent Co trimer, the Co_3−PILC is insensitive to X-ray irradiation, and in agreement with elemental analysis data, no chlorine impurities were detected (Table 7). Because of the position, $2p_{1/2}-2p_{3/2}$ separation (16.1 eV), and satellite separation (4.9 eV) from the $2p_{3/2}$ peak, the XPS spectrum in Figure 10D indicates a Co speciation of Co(II) in a highly distorted octahedral coordination. Thus this XPS data indicate that a reduction of $[Co_3(OC_2H_4NH_2)_6]^{3+}$ to its divalent analogue $[Co_3(OC_2H_4NH_2)_6]^{2+}$ has occurred during the pillaring of a sample of Texas montmorillonite in ACN.

Discussion and Conclusions

Smectites, such as montmorillonite, hectorite, and saponite, were pillared in different solvents (methanol, water, and acetonitrile) with cationic species containing clusters of one to three cobalt ions separated by bridging ligands. Solutions of the $[Co_3(OCH_2CH_2NH_2)_6](ClO_4)_3$ salt were determined to be stable by UV−vis spectroscopy under lengthy reflux conditions in both acetonitrile and methanol, while in water decomposition occurred after 96 h. The trimer decomposed in neutral aqueous solution within 4 days, but appeared to be stable in an acidic aqueous system. In contrast, the dimeric cobalt species $[Co_2(OCH_2CH_2NH_2)_3(HOCH_2CH_2NH_2)_3](NO_3)_3 \cdot {}^1/_2H_2O$ and monomeric cobalt complex $[Co(OCH_2CH_2NH_2)_3]$ proved to be unstable under the synthesis conditions used. For this reason, efforts focused on the trimeric cobalt cation $[Co_3(OC_2H_4NH_2)_6]^{3+}$ and its divalent analogue $[Co_3(OC_2H_4NH_2)_6]^{2+}$ as pillaring agents for montmorillonites, a clay commercially available in large quantities.

An increase in charge density on the smectite layer did appear to allow a greater incorporation of $[Co_3(OC_2H_4NH_2)_6]^{3+}$ in ACN, the pillaring agent of choice. The relationship between trimer uptake and layer expansion was not linear. Initially, as the Co trimer is introduced, it assumed an orientation parallel with the clay silicate layer. The complex tilted somewhat at intermediate Co loadings, resting at an angle of approximately 48° relative to the interior clay surface. As Co uptake reached its upper limit, the Co complex tilted even more, resulting in a 61° incline relative to the clay surface. Clustering of the pillar is probably occurring in order to achieve this larger *d* spacing.

XRD results indicate that excess trimer can lead to crystallite formation. Molecular scale AFM images have shown the presence of impurities on the clay exterior surface believed to be trimer molecules. The nature and type of interlamellar cation, layer charge, and composition of the silicate layer can influence the Co_3−PILC structure.

Although exhibiting variance in *d* spacing at different Co loadings, thermogravimetric analyses of the various Co_3−PILC samples were all qualitatively similar. Ligand decomposition occurred in two steps in the 250−450 °C temperature range. Below 250 °C, after some partial ligand losses, pillars adopted a position parallel to the clay surface. Furthermore, the *d* spacing value changed very little over the temperature range responsible for the first ligand removal. Thus, only moderate heating is required to lay open metal sites for potential catalytic applications. However, after the second mass loss ($T >$ 400 °C), evidence of an expended structure was lost and different cobalt oxides, some with mixed valence states, were formed, depending on the final heating temperature.

The presence of the pristine trimer in air-dried Co_3−PILC samples was confirmed by FT-LRS and FT-IR spectra together with elemental analysis data. IR bands assigned to C−H and N−H stretches from the Co trimer ligands showed broadening and shifts in relative intensity after pillaring. This implied that more than one bonding environment existed for the ligands, lending support to TGA and DTA results. XPS experiments have indicated that the Co trimer has been reduced to its divalent analogue during the pillaring reaction. Thus Co_3−PILC will contain $[Co_3(OC_2H_4NH_2)_6]^{2+}$ ions having Co(II) atoms in a distorted octahedral coordination.

Smectites pillared with $[Co_3(OC_2H_4NH_2)_6]^{3+}$ ions in ACN, the solvent of choice, lack the proper stability for high-temperature (T > 400 °C) applications. However, partial decomposition of the trimeric complex can be achieved while a 0.45 nm layer expansion is maintained, indicating that these materials could be considered for low temperature (T < 200 °C) catalytic applications.

Safety Note

The perchlorate salts of the Co complex are potentially explosive and are particularly unstable when exposed to a heat source. **All perchlorate salts should be handled with great caution** [cf. *J. Chem. Educ.* **1973**, *50*, A335. *Chem. Eng. News* **1983**, *61*, 4; **1963**, *41* ,47].

Acknowledgment. Special thanks are due to Prof. A. Wilkinson (Georgia Institute of Technology) for assisting with XRD data acquisition, to Dr. M. Chopra (Hong Kong University of Science & Technology) for providing FT LRS results, and to Susan B. Occelli for preparing the manuscript.

CM9811141